Anisotropic bond percolation

1979 J. Phys. A: Math. Gen. 12 1267

(http://iopscience.iop.org/0305-4470/12/8/021)

J. Phys. A: Math. Gen., Vol. 12, No. 8, 1979. Printed in Great Britain

Anistropic bond percolation†

S Redner‡§ and H E Stanley‡

‡ Boston University, Boston, Massachusetts, USA 02215
§ University of Toronto, Toronto, Canada M5S 1A7

Received 26 September 1978

Abstract. We introduce anisotropic bond percolation in which there exist different occupation probabilities for bonds placed in different coordinate directions. We study in detail a d-dimensional hypercubical lattice, with probabilities $p_\perp$ for bonds within $(d-1)$-dimensional layers perpendicular to the z direction, and $p_\parallel \equiv Rp_\perp$ for bonds parallel to z. For this model, we calculate low-density series for the mean size S, in both two and three dimensions for arbitrary values of the anisotropy parameter R. We find that in the limit $1/R \to 0$, the model exhibits crossover between 1 and d-dimensional critical behaviour, and that the mean-size function scales in $1/R$. From both exact results and series analysis, we derive that the crossover exponent ($\equiv \phi_1$) is 1 for all d, and that the divergence of successive derivatives of S with respect to $1/R$ increases with a constant gap equal to 1 in two and three dimensions. In the opposite limit $R \to 0$, crossover between $d-1$ and d-dimensional order occurs, and from our analysis of the three-dimensional series it appears that here the crossover exponent ϕ_{d-1} is not equal to the two-dimensional mean-size exponent. This feature is in contrast with the corresponding situation in thermal critical phenomena where ϕ_{d-1} does equal the susceptibility exponent in two dimensions. Finally, our analysis appears to confirm that the value of the mean-size exponent is independent of anisotropy in accordance with universality.

1. Introduction

In recent years, the percolation problem has seen renewed and wide interest. (For reviews, see e.g. Frisch and Hammersley 1963, Shante and Kirkpatrick 1971, or Essam 1972.) Part of the reason for this interest is that there exists a mapping between percolation and a statistical mechanical model, the Potts model (Kasteleyn and Fortuin 1969), and consequently, the geometrical phase transition that occurs in percolation can be described in the language of critical phenomena. In critical phenomena, extreme importance must be attached to the fact that the study of *anisotropic* systems advanced our understanding, and that the notion of *crossover* emerged as a central part of this understanding (see e.g. Riedel and Wegner 1969, Liu and Stanley 1972, 1973, Citteur and Kasteleyn 1972, 1973, Krasnow *et al* 1973, Fisher 1974, Aharony 1976). The useful results obtained from these studies lead us to consider the effect of anisotropy on percolation. In this article, we study an anisotropic bond percolation problem on a d-dimensional hypercubical lattice, in which the occupation probability for bonds lying within $(d-1)$-dimensional layers perpendicular to z is $p_\perp$, while bonds parallel to z are occupied with probability $p_\parallel \equiv Rp_\perp$. While this model has been considered previously mainly for $d = 2$ (Sykes and Essam 1963, Temperley and Lieb 1971), our work is the first detailed treatment of the problem for all d. We have also calculated low-density

† Work supported in part by NSF and AFOSR, and ARO.

0305-4470/79/081267+17$01.00

series for the mean-size for the two- and three-dimensional models to order 12 and 8 respectively, for arbitrary values of the anisotropy strength. These series have been analysed to map out the phase diagram (see figure 1) and to study a variety of features of the model.

For this model system, we are particularly interested in studying crossover, and there are two types which may be considered. The first is crossover between 1 and d-dimensional ordering near the one-dimensional critical point, $1/R = 0$. This corresponds to quasi-one-dimensional behaviour in magnetism (Birgeneau *et al* 1971). In this case, the crossover exponent ($\equiv\phi_1$) is shown to be 1 for all d by exploiting exact results that we derive for the derivative of the mean-size with respect to the inverse of the anisotropy strength $1/R$. Moreover, in the neighbourhood of $1/R = 0$, our series analysis indicates that the mean-size, and hence all percolation functions (Essam and Gwilym 1971), scale in $1/R$.

The second type of crossover is between $d-1$ and d-dimensional ordering about the $(d-1)$-dimensional critical point $R=0$. This case has an analogy with quasi-two-dimensional magnetic behaviour (Birgeneau *et al* 1969, de Jongh and Miedema 1974). In this case, our analysis does not yield quantitative predictions, although it appears that here, the crossover exponent ϕ_{d-1} is not equal to the mean-size exponent in $d-1$ dimensions. This is in contrast with what occurs in thermal critical phenomena, where ϕ_{d-1} does equal the $(d-1)$-dimensional susceptibility exponent† (Abe 1970, Suzuki 1971, Liu and Stanley 1972, 1973, Citteur and Kasteleyn 1972, 1973).

In addition, we have analysed our series to find the mean-size exponent γ. We find that the value of γ varies by less than 10% for $0{\cdot}1 \leqslant R \leqslant 10$ in two dimensions, and for $0{\cdot}1 \leqslant R \leqslant 6$ in three dimensions. While we expect that exponent estimates based on analysing finite-length series will show some dependence on R, past work has shown that this dependence is not physical (Rapaport 1971, Paul and Stanley 1972), and we may thus infer that the exponent is in fact independent of R, in accordance with universality.

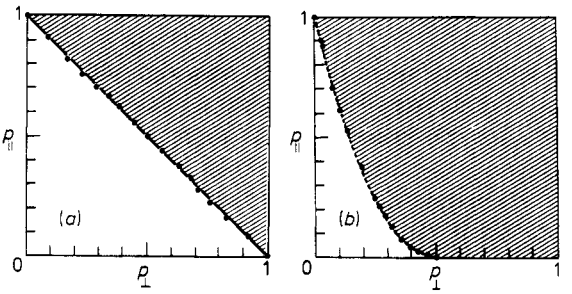

Figure 1. The phase diagrams for anisotropic bond percolation in two dimensions (a), and three dimensions (b). The shaded region represents the percolating region as a function of $p_{\|}$ and $p_{\perp}$. In (a) the exact result $p_{\|}+p_{\perp}=1$ (Sykes and Essam 1963) is represented by the full line.

2. Series calculation

The calculation of the mean cluster size in a low density series is based on enumerating all clusters containing b bonds, in which $b_{\perp}$ of them lie within the $(d-1)$-dimensional

† The susceptibility is the analogue of the mean-size in percolation.

layers (the x–y plane for $d = 3$), and $b_\parallel = b - b_\perp$ bonds are parallel to z (this method of applying series expansions to percolation was first suggested by de Gennes *et al* (1959), and by (Domb 1959)). Each cluster of occupied bonds must be surrounded by unoccupied bonds in order to isolate the cluster from the rest of the lattice. For illustration we show in figure 2, clusters of one and two bonds that occur in three dimensions, and the contribution of each to the expectation value of the number of clusters with b bonds, denoted by $\langle n_b \rangle$. In general, we may write $\langle n_b \rangle$ in the form,

$$\langle n_b \rangle = \sum_{\substack{b_\perp, b_\parallel \\ b_\perp + b_\parallel = b}}^{b} p_\perp^{b_\perp} p_\parallel^{b_\parallel} D_{b_\perp b_\parallel}(q_\perp, q_\parallel) \tag{2.1}$$

where $q = 1 - p$, and the perimeter polynomial, $D_{b_\perp b_\parallel}$ is a convenient way of characterising the boundaries for clusters of a given bond size (see e.g. Sykes and Glen 1976).

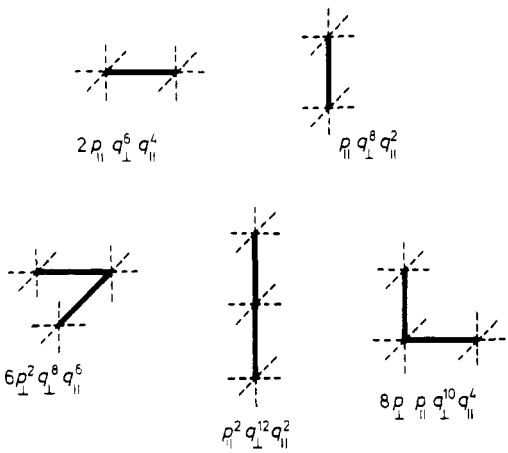

Figure 2. Representative clusters containing one and two bonds which occur in anisotropic bond percolation. The full lines represent occupied bonds, and the broken lines indicate the perimeter bonds. Each cluster contributes to a unique term in $\langle n_b \rangle$ as indicated.

We have used computer methods to calculate the $\langle n_b \rangle$ by generalising the algorithm described by Martin (1974) to allow for the case of spatial anisotropy. With these techniques, we have enumerated all clusters of up to 12 bonds in two dimensions and 8 bonds in three dimensions. From our computer data, the mean-size $S(p_\perp, p_\parallel)$ at low densities may be found by the weighted average,

$$S(p_\perp, p_\parallel) = \sum_b b^2 \langle n_b \rangle / \sum_b b \langle n_b \rangle. \tag{2.2}$$

The quantity $\Sigma_b\, b\langle n_b \rangle$ is simply the probability that a bond is occupied and we may therefore write,

$$\begin{aligned} \{(d-1)p_\perp + p_\parallel\} S(p_\perp, p_\parallel) &= \sum_{b=1}^{\infty} b^2 \langle n_b \rangle \\ &= \sum_{\substack{b_\perp = 1 \\ b_\perp + b_\parallel = b}}^{\infty} \sum_{b_\parallel = 1}^{\infty} b^2 p_\perp^{b_\perp} p_\parallel^{b_\parallel} D_{b_\perp b_\parallel}(q_\perp, q_\parallel) \\ &\equiv \sum \sum A_{b_\perp b_\parallel} p_\perp^{b_\perp} p_\parallel^{b_\parallel}. \end{aligned} \tag{2.3}$$

In the third line of (2.3), the perimeter polynomial has been expanded in powers of p. Due to the factors of p on the left-hand side of (2.3), the calculation of the mean-size series to order N, requires cluster configurational data to order $N+1$. However, if one calculates the series for $\Sigma\, b\langle n_b\rangle$ in addition, then the sum rule $\Sigma\, b\langle n_b\rangle = (d-1)p_\perp + p_\parallel$ can be exploited to yield an additional term in the series for S without further cluster enumeration (see (2.6) of Sykes and Glen 1976 for details). In this way we have calculated the mean-size series to order 12 in two dimensions, and to order 8 in three dimensions; the series coefficients are shown in tables 1 and 2.

3. Discussion and exact results

From the tables we readily verify that in the limiting cases of $R = 0$ and $R = 1$, we obtain the isotropic mean-size series for dimensions $d-1$ and d respectively, and that the case $1/R = 0$ gives the one-dimensional series. In addition, we notice a striking feature in that the coefficients A_{1l} multiplying the factor $p_\perp p_\parallel^l$ (i.e. the series for $\partial S/\partial(1/R)|_{1/R=0}$) are successive multiples of 8. We shall show that the crossover exponent ϕ_1 may be determined by the large l behaviour of the A_{1l}, and moreover the verification of these coefficients provides a strong check on the computer calculation. For these reasons, we are motivated to evaluate the A_{1l} exactly. Our computation shows that important differences exist between the effect of anisotropy in percolation and in the corresponding thermal problem. These differences can be made apparent by employing two

Table 1. The coefficients $A_{b_\perp b_\parallel}$ of the two-dimensional mean-size series defined by,

$$(p_\perp + p_\parallel)S(p_\perp, p_\parallel) = \sum_{\substack{b_\perp \\ b_\perp + b_\parallel = b}} \sum_{b_\parallel} A_{b_\perp b_\parallel} p_\perp^{b_\perp} p_\parallel^{b_\parallel}.$$

Here $p_\perp$ and $p_\parallel$ are the occupation probabilities for bonds lying in the x- and z-directions respectively. Notice that the 1st row and 1st column are the one-dimensional mean-size series, while one-half of the sum of the diagonal entries (lower left to upper right) are the terms in the isotropic two-dimensional series. Furthermore, the entries in the 2nd row and 2nd column are multiples of 8, from which we deduce that the crossover exponent in two dimensions is 1 (see text for more detail).

$b_\perp$ \ $b_\parallel$	0	1	2	3	4	5	6	7	8	9	10	11	12	13
0	0	1	2	2	2	2	2	2	2	2	2	2	2	2
1	1	8	16	24	32	40	48	56	64	72	80	88	96	
2	2	16	44	92	142	228	292	424	494	680	748	996		
3	2	24	92	232	484	824	1392	1984	3032	3896	5620			
4	2	32	142	484	988	2334	3504	7066	8968	16788				
5	2	40	228	824	2334	5224	11128	19984	36930					
6	2	48	292	1392	3504	11128	18744	50940						
7	2	56	424	1984	7066	19984	50940							
8	2	64	494	3032	8968	36930								
9	2	72	680	3896	16788									
10	2	80	748	5620										
11	2	88	996											
12	2	96												
13	2													

Table 2. The coefficients $A_{b_\perp b_\parallel}$ of the three-dimensional mean-size series defined by,

$$(2p_\perp + p_\parallel)S(p_\perp, p_\parallel) = \sum_{\substack{b_\perp \\ b_\perp + b_\parallel = b}} \sum_{b_\parallel} A_{b_\perp b_\parallel} p^{b_\perp} p^{b_\parallel}.$$

Here $p_\perp$ and $p_\parallel$ are the occupation probabilities for bonds lying in the x–y plane and z-directions respectively. Notice the following limiting cases: the first row is the one-dimensional series, one-half of the first column is the isotropic two-dimensional series, and one-third of the sum of the diagonal elements gives the isotropic three-dimensional series. Furthermore, the entries in the second row are multiples of 16, from which we deduce that $\phi_1 = 1$ in three dimensions (see text).

$b_\perp$ \ $b_\parallel$	0	1	2	3	4	5	6	7	8	9
0	0	1	2	2	2	2	2	2	2	2
1	2	16	32	48	64	80	96	112	128	
2	12	80	232	488	812	1272	1752	2432		
3	36	336	1304	3504	7432	13616	22688			
4	96	1232	5820	19704	48240	107396				
5	252	4176	24488	97920	289412					
6	600	13168	89736	431592						
7	1524	39808	327848							
8	3336	114752								
9	8432									

different methods of calculation (for comparison with the thermal problem, see Liu and Stanley 1972, 1973, Citteur and Kasteleyn 1972, 1973).

One method is based on examining the bond clusters that appear in our computer enumeration, and picking out only those which give a contribution to the mean-size linear in $1/R$. Two types of graph occur: those with one bond in a $(d-1)$-dimensional layer and an arbitrary number of z-bonds (see figure 3(a)), and those consisting only of z-bonds (see figure 3(b)). In contrast, in the corresponding analysis for the terms linear in $1/R$ in the susceptibility, only self-avoiding-walks (SAW's), which also belong to the first class of graphs, occur.

The contribution of this first class of graph to S is

$$p_\parallel^{N-1} p_\perp q_\parallel^4 q_\perp^a N^2 e = (1/R) p_\parallel^N q_\parallel^4 q_\perp^a N^2 e \tag{3.1}$$

where N is the total number of bonds in the cluster, a is the number of in-layer perimeter bonds, and e is the number of embeddings of the cluster. The quantity e is determined by counting the number of ways that the in-layer bond can join together two adjacent chains of $N-k-1$ and k z-bonds, with k arbitrary. From figure 3(c), we see that this in-layer bond can attach to $N-k$ vertices on one side, and $k+1$ vertices on the other side. In addition, the in-layer bond can lie in $d-1$ different coordinate directions. Thus we have,

$$\begin{aligned} e &= (d-1) \sum_{k=0}^{N} (N-k)(k+1) \\ &= (d-1)N(N+1)(N+2)/6. \end{aligned} \tag{3.2}$$

In addition, since we are interested only in the contribution linear in $1/R$, the quantity $q_\perp = 1 - p_\perp = 1 - p_\parallel/R$ can be set equal to 1.

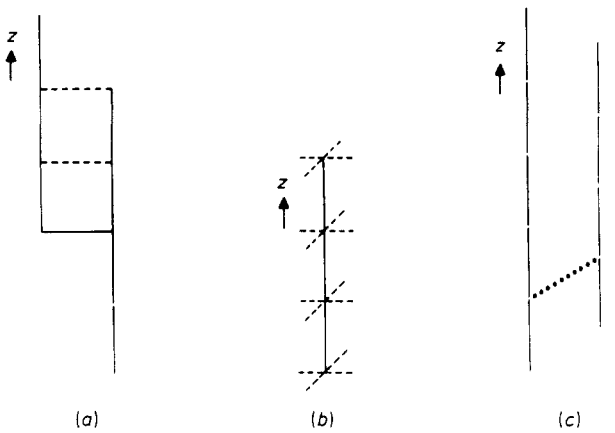

Figure 3. (*a*) One class of graphs giving a linear contribution in $1/R$ to the mean-size, due to the presence of the single in-layer bond. Notice that the contributions of the two chains of z-bonds are not independent due to shared perimeter bonds (shown broken). (*b*). The second class of graphs giving a linear contribution in $1/R$. The linear term comes from the coefficient of $p_\perp$, arising from expanding the factors of $q_\perp$ for the in-layer perimeter bonds (shown broken). (*c*). The embedding factor e for the type of graph represented in 2(*a*), may be obtained by noting that the in-layer bond (shown schematically) can attach to $N-k$ vertices on one side and $k+1$ vertices on the other side. Here N is the total number of bonds in the graph, and $0 \leq k \leq N$.

The graphs of figure 3(*b*) give a contribution to the mean-size of,

$$p_\parallel^N q_\parallel^2 q_\perp^{2(d-1)(N+1)} N^2 \tag{3.3}$$

and in the limit $1/R \to 0$, we expand q to first order in $1/R$ to obtain,

$$-(2/R)(d-1)(N+1)N^2 p_\parallel^{N+1} q_\parallel^2 + \ldots . \tag{3.4}$$

The coefficient of the mean-size series, linear in $1/R$ is the sum of (3.1) and (3.4), and after some straightforward but tedious algebra we obtain

$$\partial S/\partial(1/R)|_{1/R=0} = (d-1)p + (d-1)\sum_{N=2}^{\infty} 8(N-1)p^N \tag{3.5}$$

in agreement with our tabulated series. Notice that (3.5) may be rewritten as

$$\begin{aligned} \partial S/\partial(1/R)|_{1/R=0} &= 2(d-1)[(1+p)/(1-p)]^2 - (d-1) \\ &= (d-1)(2S_1^2 - 1) \end{aligned} \tag{3.6}$$

where S_1 is the one-dimensional mean-size. In this form the asymptotic behaviour of $\partial S/\partial(1/R)|_{1/R=0}$ is readily seen to be,

$$\begin{aligned} \partial S/\partial(1/R)|_{1/R=0} &\sim (p-p_c)^{-2} \\ &= (p-1)^{-2} \end{aligned} \tag{3.7}$$

and in the next section, we shall exploit (3.7) to deduce the value of ϕ_1.

The second method of calculating the terms linear in $1/R$ which is considerably simpler, and analogous to the methods employed in the thermal problem, is based on using the percolation analogue of the fluctuation theorem (Essam 1971, Levinshtein *et*

al 1975). Our starting point is the statement of the fluctuation theorem generalised to anisotropic bond percolation

$$(N_B/d)\{(d-1)p_\perp + p_\parallel\}S(p_\perp, p_\parallel) = \sum_{b,b'} L(b, b') \tag{3.8}$$

where N_B is the total number of lattice bonds, and $L(b, b')$ is the pair-connectedness function, defined as the probability that bonds b and b' are occupied† and joined by a connected path, and the sums on b and b' are over all bonds in the lattice. Therefore S can be found by counting all SAW's joining b and b', and subtracting off all distinct non-SAW's joining b and b'. If we are interested in $\partial S/\partial(1/R)|_{1/R=0}$ then no closed loops can occur (see figure 4) and we need to count only SAW's; therein lies the simplicity of this method.

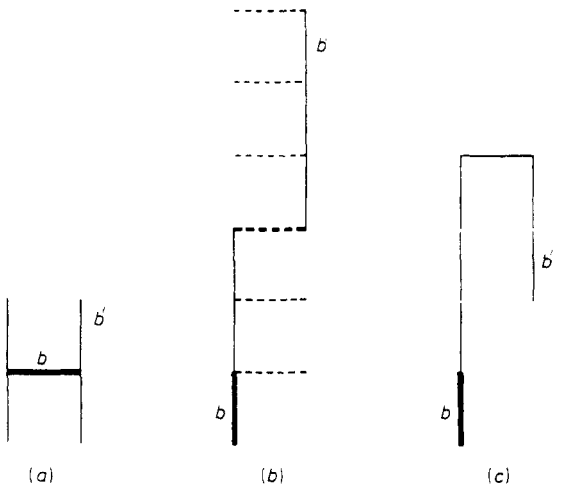

Figure 4. Graphs giving a linear contribution in $1/R$ to the pair-connectedness. The initial bond b is indicated by the bold line, and the final bond b' is also marked. In (a), b is an in-layer bond pointing in $d-1$ possible directions, and there are four ways in which a chain of z-bonds may be attached (shown schematically). In (b), bond b now points along z, and the l ways in which the in-layer bond can attach to form a SAW without a 180° turn in it are shown schematically. In (c), there are $l-1$ ways of dividing up the z-bonds to form two adjacent chains of k and $l-k$ bonds and thus construct a SAW with a 180° turn in it.

We may use translational invariance to perform the sum on b in (3.8), and we obtain

$$\{(d-1)p_\perp + p_\parallel\}S = (d-1)\sum_{b'} L(b = b_\perp, b') + \sum_{b'} L(b = b_\parallel, b') \tag{3.9}$$

where the initial bond b is restricted to lie in a $(d-1)$-dimensional layer in the first sum, and along z in the second. The contribution of the first sum is simply $4(d-1)$, corresponding to the number of ways of embedding a single in-layer bond with a chain of z-bonds attached to it (see figure 4(a)). The second sum can be broken into contributions from two types of graphs indicated in figures 4(b) and (c). In 4(b), there are l ways in which the in-layer bond can join two adjacent chains of z-bonds to form a SAW, and there is also a symmetry factor of $4(d-1)$. In 4(c), the same symmetry factor

† If one does not specify the occupancy of either b or b', then one obtains other widely used versions of the pair-connectedness which differ by one or two powers of p compared with $L(b, b')$.

occurs, and here there are $l-1$ ways of joining the two chains of z-bonds to form a SAW with a 180° turn in it. The sum of these three terms is thus $8(d-1)l$, except for the $l=0$ case in which it is easy to see that we obtain $d-1$ instead. This then reproduces the result (3.6).

Given the ease with which (3.6) is obtained using the fluctuation–dissipation theorem, it is tempting to proceed further and attempt a calculation of the coefficients A_{2l} multiplying $p_\perp^2 p_\parallel^l$ in the mean-size. From the large l behaviour of these coefficients one can verify the 'constant gap' exponent relation to be discussed in the next section. The calculation is relatively straightforward at low order, but at higher order large numbers of closed loops occur which must be subtracted off (see figure 5). Because of this complication we are unable to obtain a general expression for the A_{2l}, and we will resort to series analysis to study their asymptotic behaviour.

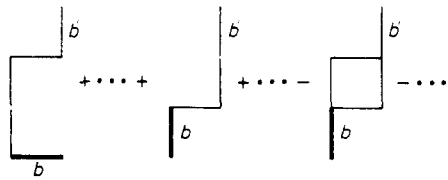

Figure 5. Typical graphs which contribute in order $p_\perp^2 p_\parallel^l$ to the pair-connectedness. At this order, there appear graphs containing closed loops, which must be subtracted from the SAW contribution.

Finally, we discuss the behaviour of the coefficients A_{l1} (i.e. the series for $\partial S/\partial R|_{R=0}$), which from the scaling relations given in the next section, determine the crossover exponent ϕ_{d-1} defined by $\partial S_d/\partial R|_{R=0} \sim (p-p_c)^{-\gamma_{d-1}-\phi_{d-1}}$. Here γ_{d-1} is the mean-size exponent in $d-1$ dimensions, and S_d is the mean size in d dimensions. While we cannot calculate $\partial S_d/\partial R|_{R=0}$ exactly, we can show that it is not equal to S_{d-1}^2, and as a result $\phi_{d-1} \neq \gamma_{d-1}$, in contrast to the thermal problem. To demonstrate this, we consider the following specific example, which for simplicity is formulated for three dimensions, but the argument can be extended to all dimensions. In figure 6(a), we show a particular graphical contribution to $\partial S_d/\partial R|_{R=0}$, consisting of four x–y bonds on one plane, and n, an arbitrary number of x–y bonds on the adjacent plane. If $\partial S_d/\partial R|_{R=0}$ were proportional to S_{d-1}^2, then the contribution of this graph would factorise into a product proportional to the fourth and nth term in the two-dimensional mean-size. The contributions to this fourth term consist of 50 SAW's minus a factor 2 corresponding to the 2 distinct ways in which closed loops may be formed with the initial bond b held fixed (see figure 6(b)). However, for the pair-connectedness graph shown, the 50 SAW's remain, but now the closed loop subtraction is larger. This is because for each of the two possible orientations of the square, there is more than one way in which the z-bond can be attached (figure 6(c)). Thus the closed loop subtraction has a somewhat three-dimensional character, and hence $\partial S_d/\partial R|_{R=0}$ does not factorise into the product of two-dimensional mean-size functions, with the result that $\phi_{d-1} \neq \gamma_{d-1}$.

4. Scaling theory and series analysis

The primary features of crossover follow from showing that the mean number of clusters (which is the percolation analogue of the Gibbs free energy), scales in the

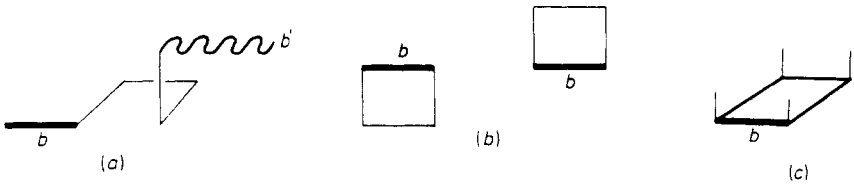

Figure 6. (*a*) A graphical contribution to the pair-connectedness consisting of four x–y bonds in one plane, one z-bond, and an arbitrary number of x–y bonds on the adjacent plane (shown schematically by the wavy line). (*b*) In two dimensions, there are two ways of forming closed loops at 4th order with bond b held fixed. When this factor of 2 is subtracted from the contribution due to 50 SAW's, we obtain the 4th term in the mean-size series. (*c*) For a graph containing the same number of bonds as in (*a*), a closed loop subtraction arises when a square occurs. For each of the two possible orientations of the square, there is more than one way that the z-bond can be attached (indicated by the thin vertical lines). As a result, the contribution to the pair-connectedness due to the four bonds on one x–y plane is less than the 4th term in the two-dimensional mean-size series.

anisotropy strength. It is toward this end that we direct our series analysis. We have introduced two types of crossover, and related to each is a distinct scaling hypothesis. Our scaling hypothesis are formulated in terms of the mean-size, as it is this function that we have calculated. From scaling of the mean-size, scaling in the mean number of clusters necessarily follows (Essam and Gwilym 1971).

The scaling hypotheses are as follows: in the vicinity of $R = 0$, we assume that the mean size is a generalised homogeneous function of $\Delta p_\perp = p_\perp - p_{\perp_c}$ and R, and hence satisfies the relation (see e.g. Hankey and Stanley 1972),

$$\lambda^{a_S} S(\lambda^{a_{p_\perp}} \Delta p_\perp, \lambda^{a_R} R) = S(\Delta p_\perp, R) \tag{4.1a}$$

where λ is arbitrary, and $a_{p_\perp}$, a_R, and a_S are the scaling powers of $\Delta p_\perp$, R, and S respectively. On the other hand, about the point $1/R = 0$ we have†

$$\lambda^{a'_S} S[\lambda^{a_{p_\parallel}} \Delta p_\parallel, \lambda^{a_{1/R}}(1/R)] = S(\Delta p_\parallel, 1/R) \tag{4.1b}$$

where $\Delta p_\parallel = p_\parallel - p_{\parallel_c}$, and $a_{p_\parallel}$, $a_{1/R}$, and a'_S are different scaling powers from those in (4.1a). The scaling relations (4.1) have important consequences which can be tested by series analysis. One is the existence of a 'constant gap' relation for the divergence of successive derivatives of S with respect to R and $1/R$. This 'constant gap' relation has been previously verified in thermal critical phenomena (see e.g. Rapaport 1971, Krasnow *et al* 1973), and to confirm the existence of a 'constant gap' for anisotropic bond percolation, we first express the divergence of S in terms of the scaling powers. We choose $\lambda = (\Delta p_\perp)^{-1/a_{p_\perp}}$ and set $R = 0$ in (4.1a), and similarly choose $\lambda = (\Delta p_\parallel)^{-1/a_{p_\parallel}}$ and set $1/R = 0$ in (4.1b). From these we have,

$$\begin{aligned} S(\Delta p_\perp, R = 0) &= \lambda^{a_S} S(1, 0) \\ &\sim (\Delta p_\perp)^{-a_S/a_{p_\perp}} \equiv (\Delta p_\perp)^{-\gamma_{d-1}} \end{aligned} \tag{4.2a}$$

$$\begin{aligned} S(\Delta p_\parallel, 1/R = 0) &= \lambda^{a'_S} S(1, 0) \\ &\sim (\Delta p_\parallel)^{-a'_S/a_{p_\parallel}} \equiv (\Delta p_\parallel)^{-\gamma_1} \end{aligned} \tag{4.2b}$$

† In two dimensions, the model system remains invariant under the transformation $R \leftrightarrow 1/R$, $p_\parallel \leftrightarrow p_\perp$, and consequently (4.1$a$) and (4.1$b$) become identical: $a^\parallel_S = a^\perp_S$, $a_{p_\parallel} = a_{p_\perp}$, $a_{1/R} = a_R$.

where γ_{d-1} and γ_1 are the mean-size exponents in $d-1$ and one dimensions respectively. Similar calculations for the derivatives of S with respect to R (and $1/R$) give,

$$\partial^n S/\partial R^n|_{R=0} \sim (\Delta p_\perp)^{-(a_S + n a_R)/a_{p_\perp}} \equiv (\Delta p_\perp)^{-\gamma_{d-1}^{(n)}} \tag{4.3a}$$

$$\partial^n S/\partial (1/R)^n|_{1/R=0} \sim (\Delta p_\parallel)^{-(a_S' + n a_{1/R})/a_{p_\parallel}} \equiv (\Delta p_\parallel)^{-\gamma_1^{(n)}}.$$

That is, the divergence of successive derivatives of S increases with a 'constant gap',

$$\gamma_{d-1}^{(n)} \equiv \gamma_{d-1} + n\phi_{d-1} \tag{4.4a}$$

$$\gamma_1^{(n)} \equiv \gamma_1 + n\phi_1 \tag{4.4b}$$

and these formulae define the crossover exponents ϕ_{d-1} and ϕ_1.

The exponent relation (4.4b) can be partially verified by using the exact result (3.6) which states

$$\partial^2 S/\partial (1/R)^2|_{1/R=0} \sim (\Delta p_\parallel)^{-2} = (\Delta p_\parallel)^{-\gamma_1^{(1)}}. \tag{4.5}$$

Since it is known rigorously that $\gamma_1 = 1$ (see Reynolds *et al* 1977 and references therein), it immediately follows that (4.4b) is valid for $n = 1$. Further confirmation of the 'constant gap' comes from a Padé analysis of $\partial^n S/\partial (1/R)^n|_{1/R=0}$. In figure 7($a$) we plot the value of the exponent versus the location of the associated singularity for the various Padé approximants to the series. For the two-dimensional case, the singularities are clustered in the vicinity of $p_\parallel = 1$ and it appears quite convincing that $\gamma_1^{(2)}$ is 3 and $\gamma_1^{(3)}$ is 4. In three dimensions there are a few singularities in the vicinity of $p_\parallel = 1$ for the second derivative series, but the higher derivative series are too short to be usefully analysed. For the second derivative, it appears quite plausible that $\gamma_1^{(2)} = 3$, in agreement with the

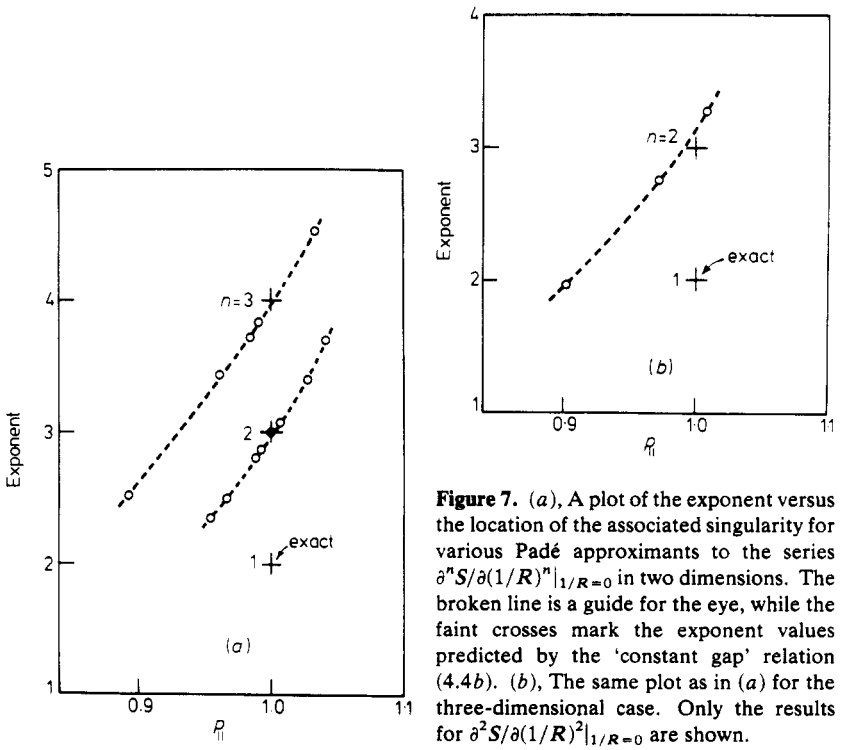

Figure 7. (a), A plot of the exponent versus the location of the associated singularity for various Padé approximants to the series $\partial^n S/\partial (1/R)^n|_{1/R=0}$ in two dimensions. The broken line is a guide for the eye, while the faint crosses mark the exponent values predicted by the 'constant gap' relation (4.4b). (b), The same plot as in (a) for the three-dimensional case. Only the results for $\partial^2 S/\partial (1/R)^2|_{1/R=0}$ are shown.

'constant gap' relation (see figure 7(*b*)). Thus for the cases considered, our analysis supports the validity of the scaling hypothesis in the quasi-one-dimensional regime.

We next turn to a study of the crossover exponent ϕ_{d-1}, by performing a Padé analysis of the three-dimensional series for $\partial^n S/\partial R^n|_{R=0}$. Our results are shown on an exponent versus location plot in figure 8 (Sykes *et al* 1976a). From the figure, it appears that the exponent for the 2nd, 3rd, and 4th derivatives of S differ approximately by a constant amount of 1·75. If we in addition approximate γ_2 by 2·5 and invoke the 'constant gap' relation, we then expect the exponent of $\partial S/\partial R$ to be 4·25. This is not consistent with our Padé analysis, and we anticipate that longer series would resolve the situation.

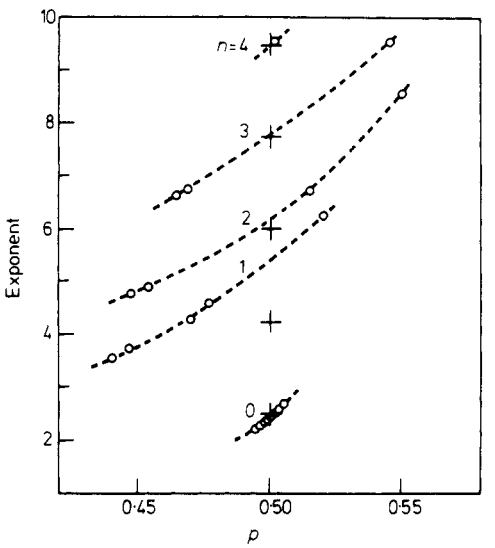

Figure 8. A similar plot to those in figure 5 except the analysis is for the series $\partial^n S/\partial R^n|_{R=0}$ in three dimensions. The faint crosses mark the exponent values predicted by the 'constant gap' relation (4.4*a*) assuming $\phi_{d-1}=1{\cdot}75$ and $\gamma_{d-1}=2{\cdot}5$.

We can gain further information about the crossover exponents by mapping out the phase diagrams and investigating the singular behaviour of the quantities $p_{\perp_c}(R)-p_{\perp_c}(R=0)$ and $p_{\|_c}(1/R)-p_{\|_c}(1/R=0)$ as the system crosses over between universality classes (Riedel and Wegner 1969). The scaling relations (4.1) predict that near $R=0$, the critical concentration varies as,

$$|p_{\perp_c}(R)-p_{\perp_c}(R=0)|\sim R^{1/\phi_{d-1}} \tag{4.6a}$$

while near $1/R=0$ we have,

$$|p_{\|_c}(1/R)-p_{\|_c}(1/R=0)|\sim(1/R)^{1/\phi_1}. \tag{4.6b}$$

In two dimensions the crossover exponents can be deduced from (4.6) by applying the exact result (Sykes and Essam 1963),

$$p_{\perp_c}+p_{\|_c}=1 \tag{4.7}$$

where $p_{\perp_c}$ and $p_{\|_c}$ are the critical concentrations in the x and z directions respectively. From (4.6) and (4.7), it follows immediately that $\phi_{d-1}=\phi_1=1$.

Since we are ultimately interested in determining the crossover exponent ϕ_{d-1} in three dimensions using (4.6*a*), it is imperative to calculate $p_c(R)$ accurately. Therefore we have used (4.7) as a check by which we have tested analysis techniques for the two-dimensional series. In this way, we have obtained methods which we have then applied to the three-dimensional series with great confidence.

The essential difficulty in applying any analysis method stems from the fact that low-density series in percolation eventually converge to a non-physical singularity at negative values of p, which is closer to the origin than the physical singularity (Sykes *et al* 1973). Thus it is often the case that beyond a certain order l_0, estimates of critical properties based on a ratio analysis become quite erratic. However, for orders $l < l_0$, the remaining ratios can sometimes be usefully extrapolated to yield information about the physical singularity.

To illustrate, we consider the two-dimensional isotropic series ($R = 1$), for which 14 terms have been calculated by Sykes and Glen (1976). In figure 9(*a*) we plot against $1/l$, the lth estimate for the critical point $cp_l \equiv l\rho_l - (l-1)\rho_{l-1}$, based on a linear extrapolation of the ratios of successive series coefficients $\rho_l = a_l/a_{l-1}$. These estimates exhibit large oscillations which can be substantially reduced by forming the critical point estimates $\overline{cp}_l$ found by linearly extrapolating the 'square root' ratios $\bar{\rho}_l = (a_l/a_{l-2})^{1/2}$. Further progress can be made by now studying the successive averages $d_l \equiv (\overline{cp}_l + \overline{cp}_{l-1})/2$ as a function of $1/l$. (Similar techniques are described in Gaunt and Guttman 1974 and references therein.) For $l \leqslant 11$, the d_l converge quite accurately to the exact critical point of 0·5. However, for $l > 11$, large oscillations in the d_l appear, due to the asymptotic dominance of the non-physical singularity, and consequently we shall ignore these last few data points (see figure 9(*b*)). For the anisotropic two-dimensional series in the range $0{\cdot}4 < R < 1$, this dependence of the d_l on $1/l$ persists (figure 9(*c*)), and we have exploited this fact to estimate the critical concentration to within 1% agreement of the exact result, as indicated in table 3. For decreasing $R < 0{\cdot}4$, the relative influence of the non-physical singularity diminishes, and the smoothed critical point estimates now behave regularly at the last order, leading to even more accurate results (figure 9(*d*)).

Similar considerations apply in estimating the mean-size exponent γ. The oscillations in the ratio estimates can be greatly reduced by suitable averaging procedures, although here the Padé technique gives better results, and we thereby find that γ varies by less than 10% for $0{\cdot}1 \leqslant R \leqslant 10$ as shown in table 3. For small R, the apparent non-universality of γ occurs because the critical region shrinks as R decreases, and correspondingly more series terms are required to make the true two-dimensional character of the phase transition evident (Rapaport 1971, Paul and Stanley 1972).

Now that we have demonstrated the usefulness of our analysis methods in two dimensions, we turn our attention to the three-dimensional series. As an initial trial, we consider the ten-term isotropic series calculated by Sykes *et al* (1976b). By studying the smoothed critical point estimates d_l, we obtain the result $p_c = 0{\cdot}247 \pm 0{\cdot}0005$ as indicated in figure 10. It is evident that the averaging procedure works remarkably well, and moreover the influence of the non-physical singularity is less important than in two dimensions, at the last order presently available. Our anisotropic series have eight terms however, and while accurate results can be obtained for $R \cong 0$ and $R \cong 1$ by using the longer isotropic series as a guide, our estimates of $p_c(R)$ are typically more uncertain than in two dimensions (see table 4). In contrast, it is much easier to obtain estimates for the mean-size exponent than in two dimensions, and it appears that γ is essentially constant for $0{\cdot}1 \leqslant R \leqslant 6$.

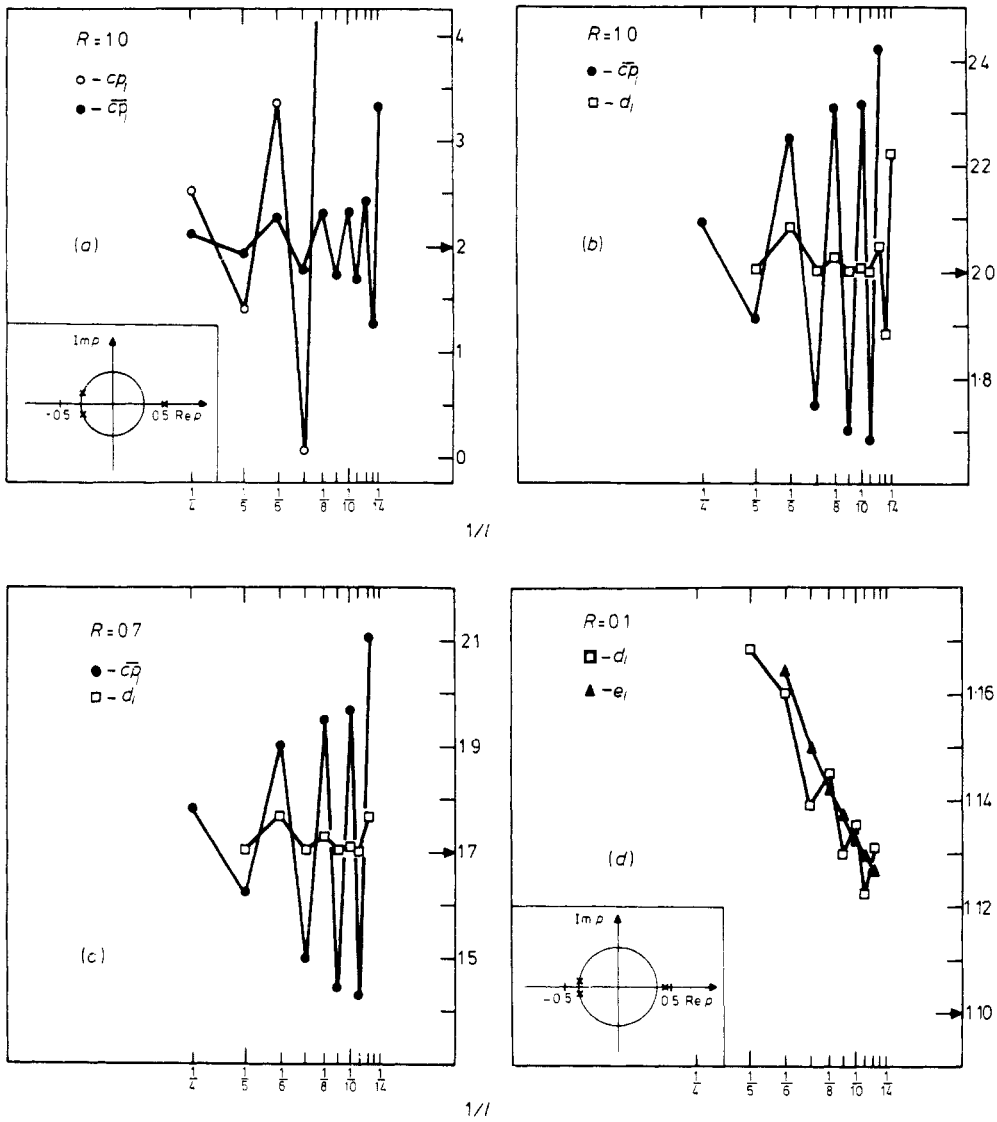

Figure 9. (*a*), Critical point estimates based on a ratio analysis of the terms in the two-dimensional isotropic bond series. Shown are the *l*th estimate for the critical point cp_l, based on a linear extrapolation of the ratios ρ_l (which go off scale at 8th order), and the $\overline{cp}_l$ based on linearly extrapolating the $\tilde{\rho}_l$. The data points are joined to serve as a guide for the eye. In addition, the exact limiting behaviour is indicated by the arrow on the right. The inset shows the approximate locations of the physical and non-physical singularities, and the radius of convergence in the complex p plane. (Compare with the inset in (*d*)). (*b*), For comparison with (*a*), we again show the $\overline{cp}_l$, versus $1/l$, and also the 'smoothed' critical estimates d_l. For $l \leq 11$, the d_l appear to converge quite accurately to the exact value of 2. (*c*), The same plot as (*b*) for the case $R = 0{\cdot}7$. Notice again that for $l \leq 11$, the d_l appear to converge to the exact limit of 1·7. (*d*), For $R = 0{\cdot}1$, we plot both d_l and the 2nd successive averages $e_l \equiv (d_l + d_{l-1})/2$ versus $1/l$. Since the relative importance of the non-physical singularity is reduced compared to the case $R = 1.0$ (see inset and compare with (*a*)), the d_l are nicely behaved even at 12th order, and the 2nd successive average gives extremely accurate results.

Table 3. Estimates of the critical concentration $p_{\perp c}$ and meansize exponent γ in two dimensions, for various values of R. The values of $p_{\perp c}$ given are based on the ratio method, and on the exact result (4.7) for the sake of comparison. The values of γ listed are based on an 'exponent versus location' plot of the physical singularity in the various Padé approximants (figure 8(*a*)).

R	$p_{\perp c}(R)$ Exact	$p_{\perp c}(R)$ Ratio estimates	γ Padé estimates
0·1	0·9090...	0·909 ± 0·002	2·19
0·2	0·8333 ..	0·824 ± 0·006	2·31
0·3	0·7692...	0·760 ± 0·008	2·41
0·4	0·7142...	0·710 ± 0·008	2·439
0·5	0·6666...	0·670 ± 0·005	2·408
0·6	0·6250...	0·630 ± 0·005	2·423
0·7	0·5882...	0·587 ± 0·005	2·439
0·8	0·5555...	0·553 ± 0·002	2·456
0·9	0·5263...	0·528 ± 0·002	2·444
1·0	0·5000...	0·500 ± 0·002	2·441

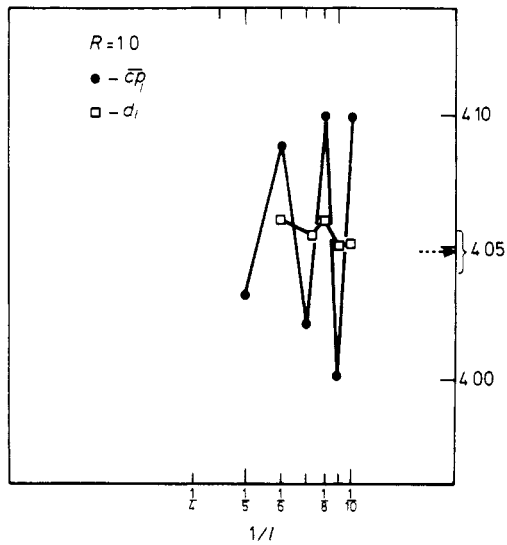

Figure 10. Critical point estimates for the isotropic three-dimensional series. Shown are $\overline{cp}_l$ and d_l versus $1/l$. The broken line on the right marks the estimate for p_c quoted in the text, while the parenthesis indicates our error estimate.

Now we are in a position to study the crossover regime for the three-dimensional system by examining $|p_c(R) - p_c(R=0)|$ for small R, and $|p_c(1/R) - p_c(1/R=0)|$ for small $1/R$. When these quantities are plotted on a log–log scale, equation (4.6) predicts that within the scaling region the data will be linear with a slope equal to the inverse crossover exponent. Consider now the small $1/R$ region; here the data show a large linear range of unit slope, consistent with $\phi_1 = 1$. One must exercise some caution in drawing conclusions, however, because in the limit $1/R \to 0$ we may neglect the second and higher powers of $1/R$ in the series, and consequently estimates for p_c necessarily depend linearly on $1/R$. As a result, the conclusion $\phi_1 = 1$ would be obtained

Table 4. Estmates of $p_{\perp c}$ and γ in three dimensions using ratio methods. The $R = 1$ entry is based on the tenth order series of Sykes *et al* (1976b), while the remaining entries are based on our eighth-order series.

R	$p_{\perp c}(R)$	γ
0·1	0·390 ± 0·003	1·61
2	0·356 ± 0·005	1·61
3	0·334 ± 0·007	1·63
4	0·315 ± 0·007	1·64
5	0·305 ± 0·005	1·65
6	0·286 ± 0·002	1·65
7	0·275 ± 0·001	1·65
8	0·264 ± 0·001	1·65
9	0·255 ± 0·001	1·65
1·0	0·247 ± 0·0005	1·66
2·0	0·188 ± 0·002	1·65
4·0	0·131 ± 0·002	1·61
6·0	0·101 ± 0·002	1·53
8·0	0·083 ± 0·002	1·47

erroneously. However, our data exhibit linearity with unit slope until $R \sim 0{\cdot}05$ (figure 11), at which point the higher powers of $1/R$ dominate in the last few series terms. Therefore we are not merely observing the manifestation of a linear approximation, but rather true scaling behaviour.

In the opposite limit, we find that for $R \leqslant 0{\cdot}01$, a linear approximation for each series term is quite accurate and this then leads to a linear dependence of $p_{\perp c}(R)$ on R. For $R \geqslant 0{\cdot}01$, a sufficient number of powers of R contribute to the series for scaling to be evident (Harbus and Stanley 1973). However, in this region the data lie on a smooth curve which asymptotically approaches a horizontal line as $R \to \infty$, as shown in the

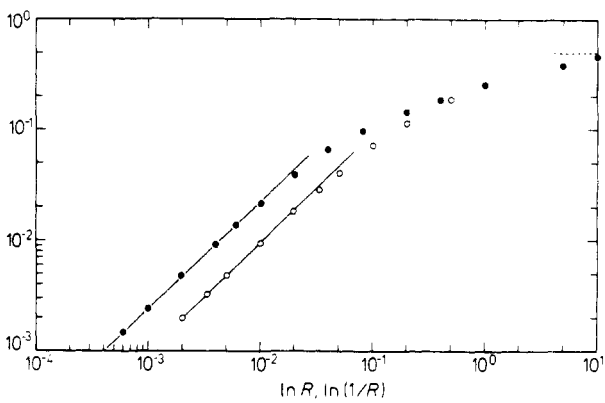

Figure 11. Dependence of $|p_{\perp c}(R) - p_{\perp c}(R=0)|$ on ln R (dots), and $|p_{\perp c}(1/R) - p_{\perp c}(1/R=0)|$ on ln $1/R$ (open circles), for the three-dimensional series. We have displayed the large R data in terms of $p_{\perp}$ rather than $p_{\parallel}$ because the relative error bars are an order of magnitude smaller and lie within the data points. The straight lines have slope unity, and the linear range of the large R data extends into the scaling region which confirms the result $\phi_1 = 1$ (see text). The linear range of the small R data occurs only outside the scaling region, and the limiting behaviour of the data as $R \to \infty$ is indicated by the horizontal dotted line on the right.

figure. Hence this plot does not yield a determination of ϕ_{d-1}. Since we are confident in the accuracy of our estimates for $p_{\perp_c}(R)$, we believe that the shortcoming of the method here is due to the smallness of the crossover regime. This would be corroborated by the apparent difficulties in the Padé analysis of the series for $\partial S/\partial R|_{R=0}$ in three dimensions.

5. Summary

We have introduced anisotropic bond percolation, and a model system exhibiting uniaxial anisotropy has been studied in detail. Low-density series for the mean-size have been calculated to order 12 and 8 in two and three dimensions respectively. The derivative of the mean-size with respect to the inverse anisotropy parameter has been calculated exactly in all dimensions, d. This yields an extremely useful check on our series calculation, and also leads to the result that the crossover exponent $\phi_1 = 1$ for all d. Series analysis has been used to verify some of the predictions of the scaling hypothesis for anisotropic systems. In particular, in the quasi-one-dimensional regime we have confirmed the validity of the 'constant gap' scaling form,

$$\partial^n S/\partial(1/R)^n|_{1/R=0} \sim (p_\parallel - p_{\parallel_c})^{-\gamma_1 - n\phi_1} \tag{5.1}$$

for both $d = 2$ and 3, while in the quasi-$(d-1)$-dimensional regime we have tentative evidence that the scaling form,

$$\partial^n S/\partial R^n|_{R=0} \sim (p_\perp - p_{\perp_c})^{-\gamma_{d-1} - n\phi_{d-1}} \tag{5.2}$$

holds for $d = 3$, where $\gamma_{d-1} = 2{\cdot}43$ and $\phi_{d-1} \cong 1{\cdot}75$. We have also mapped out the phase diagrams for the two- and three-dimensional models, and find that to within the errors inherent in the series method, the mean-size exponent is independent of the anisotropy, in agreement with universality.

Acknowledgments

The authors wish to thank Professors A Coniglio and W Klein, and Dr P J Reynolds for useful discussions. We are also grateful to Professor M B Walker who generously supplied us with computer time in order to aid the completion of this project.

References

Abe R 1970 *Prog. Theor. Phys.* **44** 339–47
Aharony A 1976 in *Phase Transitions and Critical Phenomena* vol 6 eds C Domb and M S Green (New York: Academic) pp 357–424
Birgeneau R J, Guggenhein H J and Shirane G 1964 *Phys. Rev. Lett.* **22** 720–3
Birgeneau R J, Dingle R, Hutchings M T, Shirane G and Holt S L 1971 *Phys. Rev. Lett.* **26** 718–21
Citteur C A W and Kasteleyn P W 1972 *Phys. Lett.* A **42** 143–4
—— 1973 *Physica* **68** 491–510
Domb C 1959 *Nature* **184** 509
Essam J W 1971 *J. Math. Phys.* **12** 874–82
—— 1972 in *Phase Transitions and Critical Phenomena* vol 2 eds C Domb and M S Green (New York: Academic) pp 197–270

Essam J W and Gwilym K M 1971 *J. Phys. C: Solid St. Phys.* **4** L228–32
Fisher M E 1974 *Rev. Mod. Phys.* **46** 597–616
Frisch H L and Hammersley J M 1963 *J. Soc. Indust. Appl. Math.* **11** 894–918
Gaunt D S and Guttman A J 1974 in *Phase Transitions and Critical Phenomena*, vol 3 eds C Domb and M S Green (New York: Academic) pp 181–243
de Gennes P G, Lafore P and Millot J P 1959 *J. Chem. Phys. Sol.* **11** 105–10
Hankey A M A and Stanley H E 1972 *Phys. Rev.* B **6** 3515–42
Harbus F I and Stanley H E 1973 *Phys. Rev.* B **8** 2268–72
de Jongh L J and Miedema A R 1974 *Adv. Phys.* **23** 1–260
Kasteleyn P W and Fortuin D M 1969 *J. Phys. Soc. Jap.* (*suppl.*) **26** 11–4
Krasnow R, Harbus F I, Liu L L and Stanley H E 1973 *Phys. Rev.* B **7** 370–9
Levinshtein M E, Shklovskii B I, Shur M S and Efros A L 1975 *Sov. Phys.—JETP* **42** 197–200
Liu L L and Stanley H E 1972 *Phys. Rev. Lett.* **29** 927–31
—— 1973 *Phys. Rev.* B **8** 2279–98
Martin J L 1974 in *Phase Transitions and Critical Phenomena* vol 3, eds C Domb and M S Green (New York: Academic) pp 77–112
Paul G and Stanley H E 1972 *Phys. Rev.* B **5** 2578–99
Rapaport D 1971 *Phys. Lett.* A **37** 347–9
Reynolds P J, Stanley H E and Klein W 1977 *J. Phys. A: Math. Gen.* **10** L203–9
Riedel E and Wegner F 1969 *Z. Phys.* **225** 195–215
Shante V K S and Kirkpatrick S 1971 *Advan. Phys.* **20** 325–57
Suzuki M 1971 *Prog. Theor. Phys.* **46** 1054–70
Sykes M F and Essam J W 1963 *Phys. Rev. Lett.* **10** 3–4
Sykes M F, Gaunt D S and Glen M 1976 *J. Phys. A: Math Gen.* **9** 97–103
—— 1976b *J. Phys. A: Math. Gen.* **9** 1705–12
Sykes M F and Glen M 1976 *J. Phys. A: Math. Gen.* **9** 87–95
Sykes M F, Martin J L and Essam J W 1973 *J. Phys. A: Math. Gen.* **6** 1306–9
Temperley H N V and Lieb E H 1971 *Proc. R. Soc.* A **322** 251–80